Editors' Suggestion

Peierls Transition in Gross-Neveu Model from Bethe Ansatz

Valdemar Melin,[1] Yuta Sekiguchi,[2] Paul Wiegmann,[3] and Konstantin Zarembo[2,4]
[1]Department of Physics, KTH Royal Institute of Technology, Stockholm, Sweden
[2]Nordita, KTH Royal Institute of Technology and Stockholm University, Stockholm, Sweden
[3]Kadanoff Center for Theoretical Physics, University of Chicago, Chicago, Illinois, USA
[4]Niels Bohr Institute, Copenhagen University, Copenhagen, Denmark

(Received 19 April 2024; revised 13 July 2024; accepted 14 August 2024; published 3 September 2024)

The two-dimensional Gross-Neveu model is anticipated to undergo a crystalline phase transition at high baryon charge densities. This conclusion is drawn from the mean-field approximation, which closely resembles models of Peierls instability. We demonstrate that this transition indeed occurs when both the rank of the symmetry group and the dimension of the particle representation contributing to the baryon density are large (the large N limit). We derive this result through the exact solution of the model, developing the large N limit of the Bethe ansatz. Our analytical construction of the large-N solution of the Bethe ansatz equations aligns perfectly with the periodic (finite-gap) solution of the Korteweg–de Vries (KdV) of the mean-field analysis.

DOI: 10.1103/PhysRevLett.133.101601

The Gross-Neveu (GN) model is a $(1+1)$-dimensional theory of N interacting Dirac fermions:

$$\mathcal{L} = \bar{\psi}_i(i\gamma^\mu\partial_\mu + \mu\gamma^0 - \sigma)\psi_i - \frac{N}{2\lambda}\sigma^2. \tag{1}$$

The Hubbard-Stratonovich field σ mediates local four-fermion interaction $(\lambda/N)(\bar{\psi}\psi)^2$ (on shell $\sigma = -(\lambda/N)\bar{\psi}\psi$). At zero chemical potential μ, the model features asymptotic freedom, spontaneous breaking of chiral symmetry, and dynamical mass generation: $m = \Lambda\lambda^{1/2(N-1)}e^{-\pi N/\lambda(N-1)}$ [1]. This makes it a compelling case study for nonperturbative effects in quantum field theory. Furthermore, the model is integrable, with a precisely known particle content, spectrum, and scattering S matrix [2,3].

The model possesses the global $O(2N)\times\mathbb{Z}_2$ symmetry, where $O(2N)$ acts on a multiplet formed by real and imaginary components of ψ_i, and $\mathbb{Z}_2$ is the chiral symmetry: $\psi_i \to \gamma^3\psi_i$, $\sigma \to -\sigma$. When the fermions are integrated out (at zero μ) the effective potential for σ has two minima at $\langle\sigma\rangle = \pm m$ leading to spontaneous breaking of chiral symmetry and fermion mass generation.

The phase diagram of the model at nonzero chemical potential is quite rich. Chiral symmetry is restored at high temperatures, whereas at lower temperatures and higher density, the system transitions into a crystalline phase [4–9]. These conclusions are drawn from the large-N approximation, which justifies the mean-field approach.

The motivation for our study is twofold: first, to elucidate the crystalline phase through a complete quantum solution using the Bethe-ansatz technique, and second, to establish a framework for a fully nonperturbative exploration of dense states that is valid *a priori* for finite N going beyond the mean field. Furthermore, the large N limit of the GN model provides insight into the intricate (or rather singular) relationship between quantum and classical integrable systems.

A spontaneous crystalline structure of the ground state of, otherwise a translational-invariant fermionic system, is a consequence of the Peierls instability [10,11], a celebrated phenomenon extensively studied in the condensed matter literature (see [12–15] and references therein). In the traditional condensed-matter setting the instability of electronic band structure is caused by an adibatic interaction between lattice phonons and electrons. The self-interaction in the GN model (1) mediated by the field σ yields the same effect. The large N plays a role of the adibatic parameter of the Peierles model. Furthermore, the real symmetry group $O(2N)$ gives rise to the *commensurate* Peierls transition. When an increase in the chemical potential pushes the Fermi energy into the conduction zone, the field σ which minimizes the fermionic energy becomes a spatial-periodic potential with a half-period completely determined by the chemical potential. The energy gain from rearranging the fermion spectrum (thankfully to the large N) exceeds the energy cost of distorting the environment described by σ. In the GN model the instability manifests itself as a complex pole in the σ propagator within a small range of momenta around $p \sim 2\mu$ [16], pointing towards transition

to a periodically modulated chiral condensate $\langle\sigma\rangle$. From a semiclassical perspective the spacially modulated chiral condensate becomes a dominant saddle point of the large-N path integral [7] above the critical chemical potential $\mu > 2m/\pi$ [4].

The mean-field value of σ appears to be the *cnoidal* wave, an exact periodic wave solution of the Korteweg–de Vries equation described by the Jacobi elliptic function $\langle\sigma(x)\rangle = mk^{1/2}\,\mathrm{sn}(x;k)$. The cnoidal wave is the simplest and the best studied instance of a special class of potentials known as finite-gap potential [17]. The spectrum of particles in such potentials possesses only a finite number of gaps. The $E \to -E$ symmetric spectrum of the Dirac equation in a cnoidal potential possesses the minimal number, two, symmetrically situated band gaps with ends at $(-\varepsilon_+, -\varepsilon_-)$ and $(\varepsilon_-, \varepsilon_+)$. The ends of the spectrum are determined solely by the chemical potential in such manner that the Fermi level is located inside one of the gaps. Furthermore, the density of states in the finite gap potential, referred to as a *spectral curve* and the wave functions of the states are also completely determined by the ends of the spectrum. In this Letter we will show how to obtain the spectral curve as a large N-limit of the Bethe ansatz solution of the full-fledged quantum GN model.

The fate of the fermionic crystal beyond the semiclassical approximation is an open question. One expects on general grounds that quantum corrections melt the crystal and the long-range order slowly decays at very large distances [18]:

$$\langle\sigma(x)\sigma(0)\rangle \sim \frac{\cos\pi\nu x}{|x|^{\frac{\alpha}{N}}}, \tag{2}$$

due to coupling to the Goldstone mode [19,20]. Here α is a parameter of order one. As detailed later, ν is the density of kinks in the ground state. This behavior occurs in the $U(N)$ version of the GN model, solvable exactly by bosonization [8]. The decay of the long-range order is invisible in the strict large-N limit, and the Bethe ansatz framework developed here may help to clarify the precise nature of the high-density phase.

The spectrum of the GN model consists of the elementary fermion, its bound states, and solitons. The solitons transform in the spinor representations of the D_N algebra because kinks of the σ field that interpolate between the two vacua harbor N topologically protected zero modes, one for each fermion flavor, that can be in 2^N internal states [21]. The mass spectrum of all particles is known exactly from the factorized scattering matrix [2]

$$m_a = m\frac{\sin\frac{\pi a}{2N-2}}{\sin\frac{\pi}{2N-2}}, \qquad m_{\mathrm{s}} = m_{\bar{\mathrm{s}}} = \frac{m}{2\sin\frac{\pi}{2N-2}}, \tag{3}$$

with $a = 1, \ldots, N-2$ enumerate the fundamental representation of $O(2N)$ labeled by nodes of the D_N Dynkin diagram. Owing to zero modes, kinks carry $N/2$ units of the baryon charge [22]. The baryon charge of the antisymmetric tensor of rank a is equal to a as it is a bound state of a vector particles:

$$\mathcal{B}_a = a, \qquad \mathcal{B}_{\mathrm{s}} = \frac{N}{2}. \tag{4}$$

Imagine now dispersing some amount $\mathcal{B} = \sum_a n_a\mathcal{B}_a + \mathcal{B}_{\mathrm{s}}n_{\mathrm{s}}$ of baryon charge with occupation numbers n_a in an otherwise empty system. The ground state energy of such state is just the activation energy $\sum_a n_a m_a + n_{\mathrm{s}}m_{\mathrm{s}}$. The smallest energy could be achieved by dispersing particles with the smallest mass-to-charge ratio. A simple inspection of (3), (4) shows that the optimal choice is kinks. In spite of their large mass kinks are most energy-efficient because they can store a large amount of baryon charge in their fermion zero modes. Kinks start to be created as soon as their chemical potential exceeds the mass: $\mu_{\mathrm{s}} > m_{\mathrm{s}}$. In terms of the chemical potential of baryons entered in (1), $\mu_{\mathrm{s}} = \mu\mathcal{B}_{\mathrm{s}} = \mu N/2$. Therefore, the kinks start to form a crystalline phase at $\mu > \mu_c$, where

$$\mu_c = \frac{\mu_{\mathrm{s}}}{\mathcal{B}_{\mathrm{s}}} = \frac{m}{N\sin\frac{\pi}{2N-2}} \overset{N\to\infty}{\simeq} \frac{2m}{\pi}. \tag{5}$$

These arguments are in agreement with the mean-field analysis [4–7].

The exact structure of the ground state is described by Bethe ansatz, which we consider here in its thermodynamic form (albeit at zero temperature) focusing on the ground state. As we already explained the ground state is formed by spinors, the kinks. Owing to integrability we are able to characterize these particles by their dispersion $\varepsilon(p)$ and to uniformize the dispersion by the rapidity $[\varepsilon(\theta), p(\theta)]$, a variable in which the scattering matrix is of the difference form $S(\theta - \theta')$. Furthermore, since the system is relativistic the dispersion is $(m_{\mathrm{s}}\cosh\theta, m_{\mathrm{s}}\sinh\theta)$. Then the density of rapidities $\rho(\theta)d\theta = dp$ of particles forming the ground states (kinks, in this case) satisfies a closed equation:

$$\rho(\theta) - \int_{-B}^{B} K(\theta-\eta)\rho(\eta)d\eta = m_{\mathrm{s}}\cosh\theta. \tag{6}$$

All states within the Fermi interval of rapidity $(-B, B)$ are occupied by the kinks. The value of B is fixed by the condition that the integral of $\rho(\theta)$ over the Fermi interval determines the total baryon density $\mathcal{B}/L = N/2\int_{-B}^{B}\rho d\theta\rho(\theta)$. The value of $\rho(\theta)$ outside the Fermi interval ($|\theta| > B$) defines the momentum of an excited state. The kernel in the integral equation originates from the scattering phase shift $2\pi i K(\theta) = d\ln S(\theta)/d\theta$, where $S(\theta)$ is the kink-to-kink S matrix restricted to the highest weight state, whose explicit form is presented below.

The energy of the kink, in turn, is given by the equation

$$\varepsilon(\theta) - \int_{-B}^{B} K(\theta-\eta)\varepsilon(\eta)d\eta = m_{\mathrm{s}}\cosh\theta - \mu_{\mathrm{s}}, \tag{7}$$

conditioned that the energy $\varepsilon(\theta)$ is negative within the Fermi interval and positive outside. At the end points the energy vanishes: $\varepsilon(\pm B)=0$, and this condition self-consistently determines the Fermi rapidity. The two equations (6) and (7) thus form a closed system, referred to as thermodynamic Bethe ansatz. Once the $\varepsilon(\theta)$ and B are found the energy $\mathcal{E}$ and the Landau potential $\Phi=\mathcal{E}-\mu\mathcal{B}$ of the ground state are found by integration:

$$\mathcal{E}=\frac{m_s}{2\pi}\int_{-B}^{B}\rho(\theta)\cosh\theta d\theta,\qquad \Phi=\frac{m_s}{2\pi}\int_{-B}^{B}\varepsilon(\theta)\cosh\theta d\theta. \tag{8}$$

These equations are applicable to any integrable relativistic system. The model-specific data are encoded in the S matrix, know in the case at hand from [3] that gives for the kernel:

$$K(\theta)=\int_{-\infty}^{+\infty}\frac{d\omega}{2\pi}e^{-i\omega\theta}\tilde{K}(\omega),$$
$$\tilde{K}(\omega)=1-\frac{e^{\frac{\pi|\omega|}{2N-2}}\left(\tanh\frac{\pi\omega}{2}+\tanh\frac{\pi\omega}{2N-2}\right)}{4\sinh\frac{\pi\omega}{2N-2}}. \tag{9}$$

One can check some general properties: the solution exists for any $\mu_s>\mu_c$, with a positive density $\rho(\theta)$ and the energy $\varepsilon(\theta)$ crossing zero linearly at the end points of the Fermi interval. The Landau potential behaves as $\Phi\sim-\delta^{3/2}$ at the activation threshold: $\delta=\mu/\mu_c-1$. From this we conclude that kinks crystallize at a second-order phase transition.

The BA equations can be easily solved numerically. At large N they can be solved analytically. Similar problems have been studied before, in particular for the GN model with the ground state formed by elementary fermions rather than kinks [23–26]. The interaction kernel is then $\mathcal{O}(1/N)$ and the equations are simply solved by iteration which starts from free particles. A very different situation occurs when the ground state is formed by kinks. In this case, the interaction is a dominant effect and the solution is nontrivial already at the leading order in $1/N$. This aspect appears similar to the solution of the large-N principal chiral field [27–29], even if an underlying physics is very different.

The BA equations for GN kinks at a small N were studied using perturbative techniques: for $N=2$ [26] and for $N=4$. The latter case, the $O(8)$ model, is special due to the external automorphisms, a "triality," making the vector and the spinor particles equivalent. The analysis of the BA equations of Refs. [25,30] then also applies to kinks upon substitution $\mu\to\mu_s=2\mu$.

We will be able to solve the BA equations because at large N the scattering phase becomes singular and is of the order of $\mathcal{O}(N)$:

$$\tilde{K}(\omega)\overset{N\to\infty}{\simeq}-N\frac{\tanh\frac{\pi\omega}{2}}{2\pi\omega}. \tag{10}$$

The first term in the lhs of (7), representing the energy of spinors outside of the Fermi interval $(-B,B)$ is then negligible, being much smaller than the scattering phase. Converting (10) to the θ representation we obtain a singular integral equation

$$\frac{1}{4\pi^2}\int_{-B}^{B}d\eta\varepsilon(\eta)\ln\coth^2\frac{\theta-\eta}{2}=\frac{m}{\pi}\cosh\theta-\frac{\mu}{2}. \tag{11}$$

Upon differentiation in θ it takes the standard form with the $1/\sinh$ kernel and can be solved by standard techniques [31]. The solution that goes to zero at the end points is

$$\varepsilon(\theta)=-2m\sqrt{\sinh^2B-\sinh^2\theta}. \tag{12}$$

This cannot be the end of the story because the BA equation and the condition $\varepsilon(B)=0$ should also fix B. This extra condition was lost upon differentiation. Going back to the original equation with the logarithmic kernel gives one extra constraint:

$$\frac{\pi\mu}{2m}=\frac{\mathbf{E}}{k},\qquad k=\frac{1}{\cosh B}, \tag{13}$$

where $\mathbf{E}\equiv\mathbf{E}(k)$ is the complete elliptic integral of the second kind (in the notations of [32]). This condition determines the Fermi rapidity B as a function of the chemical potential. Integrating (8) we get the free energy:

$$\Phi=-\frac{Nm^2\sinh^2B}{2\pi}, \tag{14}$$

or, equivalently,

$$\mathcal{E}-\mu_s\nu=-\frac{Nm^2k'^2}{\pi k^2}, \tag{15}$$

where ν is the density of kinks and $k'=\sqrt{1-k^2}=\tanh B$ is the complementary modulus of the elliptic integral.

At large densities, $\mu\gg m$, the Fermi rapidity grows logarithmically: $B\simeq\ln(2\mu/m)$, and $\Phi\simeq-N\mu^2/2\pi$ as expected for a gas of N species free fermions. This can be made more precise. Following [28] we identify B with the inverse of the running coupling: $\lambda(\mu)\equiv\pi/B$. Indeed, the β function obtained by differentiating (13) in $\ln\mu$ then coincides with the one-loop exact large-N expression up to (scheme-dependent) nonperturbative terms: $\beta=-(\lambda^2/\pi)(1+\text{series in}\,e^{-4\pi/\lambda})$. This makes B a useful measure of the interaction strength: the system is weakly coupled at asymptotically large densities and becomes strong when the Fermi interval shrinks to zero size: $B\sim\sqrt{4\delta/|\ln\delta|}$, implying $\Phi\sim-\delta/|\ln\delta|$. This seems to contradict our earlier conclusion that $\Phi\sim-\delta^{3/2}$. But the large-N approximation breaks down at $\delta\sim1/N$ (all three terms in the BA equations are then of the same order). There are thus two regimes at large-N: the logarithmic

scaling $\delta/|\ln\delta|$ further away from the critical point gives way to a milder $\delta^{3/2}$ behavior parametrically close to it.

The solution (12) defines the energy of holes. To find their dispersion we need to compute the density and then the momentum. In the large-N approximation,

$$\frac{1}{4\pi^2}\int_{-B}^{B} d\eta\,\rho(\eta)\ln\coth^2\frac{\theta-\eta}{2}=\frac{m}{\pi}\cosh\theta, \tag{16}$$

which again is solved by differentiating in θ. To maintain positivity of the density we need to allow for an inverse square root, a zero mode of the $1/\sinh$ kernel:

$$\rho(\theta)=\frac{m\sinh 2B}{c_s\sqrt{\sinh^2 B-\sinh^2\theta}}-2m\sqrt{\sinh^2 B-\sinh^2\theta}. \tag{17}$$

At finite N the density of particles and the density of exited states are smoothly glued at the edge of the interval $(-B,B)$. The singular behavior we found here is an artifact of the large N limit.

The coefficient c_s is fixed by substituting the solution back into the equation with the log kernel:

$$c_s=\frac{k'\mathbf{K}}{\mathbf{E}}, \tag{18}$$

where $\mathbf{K}$ is the complete elliptic integral of the first kind with the same $1/\cosh B$ modulus.

For the density of kinks we thus get

$$\nu\equiv\int_{-B}^{B}\frac{d\theta}{2\pi}\rho(\theta)=\frac{m}{k\mathbf{K}}=\frac{2\varepsilon_+\varepsilon_-}{\pi c_s\mu}, \tag{19}$$

where we used (13),(18) to get rid of ellipticae and introduced the notations

$$\varepsilon_+=m\cosh B,\qquad \varepsilon_-=m\sinh B. \tag{20}$$

As we shall see these parameters characterize the gap in the fermion spectrum.

The parameter ν plays a dual role. On the one hand, it defines the number density of kinks, how many of them fit in a unit of length, on the other hand, it also defines the largest momentum of a hole: because $dp/d\theta=\rho$, the latter varies between $-\pi\nu$ and $\pi\nu$.

We can find the dispersion relation of a hole by combining (12) with (17):

$$c_s dp=\frac{4\varepsilon_+\varepsilon_- - c_s\varepsilon^2}{\sqrt{(4\varepsilon_+^2-\varepsilon^2)(4\varepsilon_-^2-\varepsilon^2)}}d\varepsilon. \tag{21}$$

The curve $\varepsilon(p)$ is depicted in Fig. 1(a). The dispersion is approximately linear at small momenta:

$$\varepsilon\overset{p\to 0}{\simeq}c_s|p|, \tag{22}$$

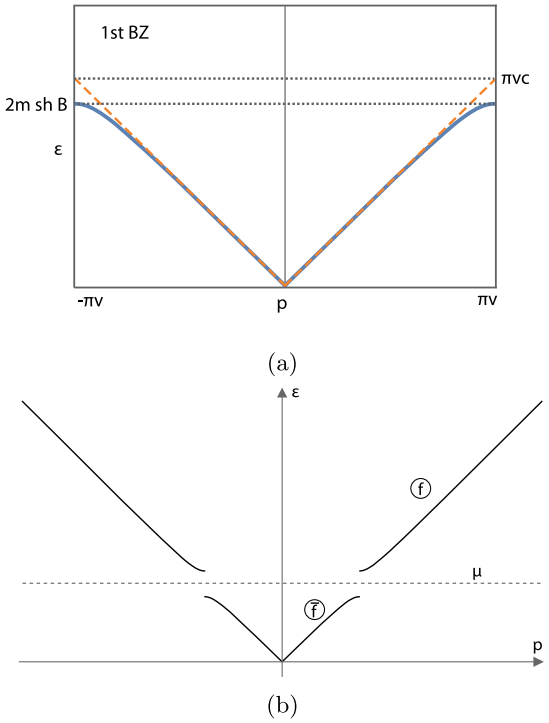

FIG. 1. The dispersion curves: (a) for the phonon; (b) the two branches of the spectral curve: The upper branch is the spectrum of vector particles (elementary fermions), the lower branch is the spectrum of holes described by kinks of opposite chirality.

as expected of the sound mode. All this suggests to identify a hole in the distribution of kinks with a phonon, the vibrational mode of the chiral crystal. The ground state can be pictured as a collection of kinks placed equidistantly as illustrated in Fig. 2. Removing one kink is equivalent to sending an acoustic wave across the lattice. Since the soliton centers are separated by $1/\nu$, the lattice vibrations naturally fit into a Brillouin zone $-\pi\nu<p<\pi\nu$, and so do the holes in the BA.

The sonic nature of the holes becomes particularly lucid at small B when $\varepsilon_+\gg\varepsilon_-,\varepsilon$, and the dispersion curve simplifies

$$c_s dp\overset{\mu\to\mu_c}{\simeq}\frac{2\varepsilon_- d\varepsilon}{\sqrt{4\varepsilon_-^2-\varepsilon^2}}. \tag{23}$$

Taking into account that $\varepsilon_+\simeq m\simeq\pi\mu/2$ and expressing ε_- from (19), we find

$$\varepsilon\overset{\mu\to\mu_c}{\simeq}2c_s\nu\left|\sin\frac{p}{2\nu}\right|, \tag{24}$$

the dispersion of a phonon in a harmonic lattice with spacing $1/\nu$. The energy is a periodic function of momentum with a period $2\pi\nu$ not only in this approximation but actually for any B. The speed of sound experiences a critical slowdown at small B: $c_s\simeq B\ln(4/B)\sim\sqrt{\delta|\ln\delta|}$, grows

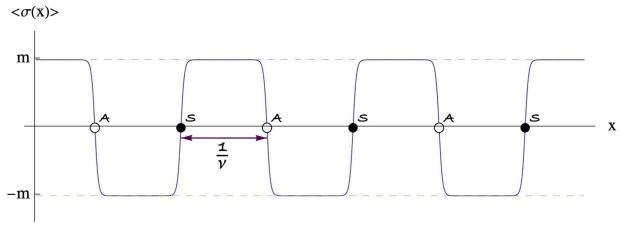

FIG. 2. The ground state as a periodic soliton.

with μ, and approaches the speed of light in the perturbative regime.

Since the soliton lattice contains two particles per unit cell (Fig. 2), the fermion Brillouin zone is half that of phonons: $-\pi\nu/2 < p < \pi\nu/2$. This fits well with the mechanics of Peierls instability [10], indeed at weak coupling (large μ) $\pi\nu \simeq 2\mu$ and the band gap opens exactly at the Fermi level. Once interactions become stronger the density of kinks ν and with it the size of the Brillouin zone diminishes faster than μ. At the critical point ($\mu \to \mu_c$) the density vanishes as $\nu \sim 1/|\ln\delta|$.

Now we turn to the part of the spectrum that corresponds to vector particles, the quanta of the fermion field in the Lagrangian (1). They do form a Fermi interval of their own, their exact energy is overall positive and is determined by the following BA equation:

$$\varepsilon_{\rm f}(\theta) - \int_{-B}^{B} d\eta K_{\rm f}(\theta-\eta)\varepsilon(\eta) = m\cosh\theta - \mu. \quad (25)$$

There is a similar equation for $dp_{\rm f}/d\theta$. In both of these equations the kernel is the derivative of the fermion-kink scattering phase [3]:

$$\tilde{K}_{\rm f}(\omega) = -\frac{e^{\frac{\pi|\omega|}{2N-2}}}{2\cosh\frac{\pi\omega}{2}}, \qquad K_{\rm f}(\theta) \overset{N\to\infty}{\simeq} -\frac{1}{2\pi\cosh\theta}. \quad (26)$$

Solving the equation at large N we find the spectral curve of an elementary fermion:

$$\varepsilon_{\rm f} = m\sqrt{\sinh^2 B + \cosh^2\theta} - \mu,$$
$$\frac{dp_{\rm f}}{d\theta} = m\sqrt{\sinh^2 B + \cosh^2\theta} - \frac{m\sinh 2B}{2c_s\sqrt{\sinh^2 B + \cosh^2\theta}}. \quad (27)$$

Excluding θ gives a differential equation:

$$c_s dp = \frac{c_s\epsilon^2 - \varepsilon_+\varepsilon_-}{\sqrt{(\epsilon^2-\varepsilon_+^2)(\epsilon^2-\varepsilon_-^2)}}d\epsilon, \qquad \epsilon = \varepsilon_{\rm f} + \mu. \quad (28)$$

Apart from fermions, we also expect to find hole-type excitations obtained by removing one fermion from the ground state. This leaves one kink with $N-1$ out of N levels filled, changing the chirality of its $O(2N)$ spinor representation. By some abuse of terminology we call kinks with one empty level antikinks. The kernel of their BA equation is determined by the scattering phase for $O(2N)$ spinor representations of opposite chirality [3]:

$$K_{\bar{\rm f}}(\omega) = K(\omega) - \frac{1}{e^{\frac{\pi|\omega|}{N-1}}+1}, \qquad K_{\bar{\rm f}}(\theta) \overset{N\to\infty}{\simeq} K(\theta) - \frac{\delta(\theta)}{2}. \quad (29)$$

Using the BA equation for the background (7) and taking into account that $\mu_{\bar{\rm f}} = \mu_{\rm s} - \mu$ we find

$$\varepsilon_{\bar{\rm f}}(\theta) = \mu + \frac{1}{2}\varepsilon(\theta), \qquad p_{\bar{\rm f}}(\theta) = \frac{1}{2}p(\theta), \quad (30)$$

for $|\theta| < B$. The energy of kinks (12) is negative inside this rapidity interval but the upward shift by μ makes the energy of antikinks overall positive.

Their spectral curve follows from (21) which, as can be easily seen, implies that the energy of antikinks satisfies the same equation (28) as the energy of fermions if we now set $\epsilon = \mu - \varepsilon_{\bar{\rm f}}$ and choose the different branch of the square root. The two branches are shown in Fig. 1(b) and together form the expected spectral curve of a Dirac fermion on the background of the periodic soliton.

It is quite remarkable that in the large N limit the fermion and antikink energies are different branches of the same elliptic spectral curve. This fact is the main aspect of the Peierls phenomenon and solely relies on the theory of periodic solutions of classical soliton equations [17]. Moreover it can be identified with the spectral curve of the mKdV equation [12] whose periodic soliton solution describes the background chiral crystal $\langle\sigma(x)\rangle$ [12,15], thus establishing direct contact between the BA and the equations of the mean-field theory. The elliptic integrals we encountered before are defined on the same elliptic curve, and one can check that the free energy (14) and the chemical potential (13) agree precisely with the predictions of the mean-field theory [15].

The common dispersion relation for fermions and holes starts linearly at small p and has a band gap at the boundary of the Brillouin zone $p = \pi\nu/2$. Indeed, the smallest fermion energy is $\varepsilon_{\rm f}(\theta=0) = \varepsilon_+ - \mu$, while the smallest hole energy is $\varepsilon_{\bar{\rm f}}(\theta=0) = \mu - \varepsilon_-$. The gap equals their sum:

$$\Delta = \varepsilon_+ - \varepsilon_- = me^{-B}. \quad (31)$$

The gap is finite at the critical point: $\Delta(\mu_c) = m$, diminishes with μ, and becomes very small at weak coupling: $\Delta \simeq m^2/(2\mu) \sim \mu e^{-2\pi/\lambda}$. This is fully nonperturbative and cannot be detected at any order of the weak-coupling expansion.

We have also solved the BA equations numerically at finite N. One conclusion we can draw from these preliminary studies is that the mean-field predictions are strikingly

robust. We can confirm that (i) the GN model undergoes a second-order Peierls transition at any $N \geqslant 2$. Once the transition is identified with the creation threshold of kinks, the critical chemical potential (5) follows from the exact mass formula. This is an exact result that does not rely on the large-N approximation. (ii) The high-density phase is characterized by a quasi-long-range crystalline order (2). Since the Bethe wave function of the ground state is translationally invariant by construction, translational symmetry is not broken. (iii) The spectrum contains a gapless phonon (also at finite N) described nonperturbatively as a hole in the Fermi sea of kinks; (iv) the fermion spectrum remains gapped at any N and any coupling strength. Our preliminary numerical studies show that $1/N$ corrections are significant and reach up to 10% even at $N = \mathcal{O}(100)$. More details on the full quantum solution of the model will be given in a separate publication.

Acknowledgments—We would like to thank Z. Bajnok, A. Balatsky, J. Balog, L. Di Pietro, V. Kazakov, D. Kuzmanovski, E. Langmann, O. Ohlsson Sax, M. Serone, F. Smirnov, E. Sobko, and D. Volin for illuminating discussions. P. W. acknowledges helpful discussions with N. Kirova and S. Brazovski. The work of P. W. was supported by the NSF under Grant No. NSF DMR-1949963. The work of K. Z. was supported by VR Grant No. 2021-04578. Nordita was partially supported by NordForsk.

[1] D. J. Gross and A. Neveu, Phys. Rev. D **10**, 3235 (1974).
[2] A. B. Zamolodchikov and A. B. Zamolodchikov, Ann. Phys. (N.Y.) **120**, 253 (1979).
[3] M. Karowski and H. J. Thun, Nucl. Phys. **B190**, 61 (1981).
[4] M. Thies and K. Urlichs, Phys. Rev. D **67**, 125015 (2003).
[5] O. Schnetz, M. Thies, and K. Urlichs, Ann. Phys. (Amsterdam) **314**, 425 (2004).
[6] M. Thies, J. Phys. A **39**, 12707 (2006).
[7] G. Basar, G. V. Dunne, and M. Thies, Phys. Rev. D **79**, 105012 (2009).
[8] R. Ciccone, L. Di Pietro, and M. Serone, Phys. Rev. Lett. **129**, 071603 (2022).
[9] R. Ciccone, L. Di Pietro, and M. Serone, J. High Energy Phys. 02 (2024) 211.
[10] R. E. Peierls, *Quantum Theory of Solids* (Oxford University Press, New York, 1955).
[11] H. Fröhlich, Proc. R. Soc. A **223**, 296 (1954).
[12] S. Brazovskii, S. Gordyunin, and N. Kirova, JETP Lett. **31**, 456 (1980).
[13] B. Horovitz, Phys. Rev. Lett. **46**, 742 (1981).
[14] M. Nakahara and K. Maki, Phys. Rev. B **24**, 1045 (1981).
[15] S. Brazovskii and N. Kirova, Sov. Sci. Rev. A **5**, 99 (1984).
[16] A. Koenigstein, L. Pannullo, S. Rechenberger, M. J. Steil, and M. Winstel, J. Phys. A **55**, 375402 (2022).
[17] S. Novikov, S. V. Manakov, L. P. Pitaevsky, and V. E. Zakharov, *Theory of Solitons. The Inverse Scattering Method* (Consultants Bureau, New York, USA, 1984).
[18] E. Witten, Nucl. Phys. **B145**, 110 (1978).
[19] V. L. Berezinskii, Sov. Phys. JETP **32**, 493 (1971).
[20] J. M. Kosterlitz and D. J. Thouless, J. Phys. C **6**, 1181 (1973).
[21] E. Witten, Nucl. Phys. **B142**, 285 (1978).
[22] R. Jackiw and C. Rebbi, Phys. Rev. D **13**, 3398 (1976).
[23] P. Forgacs, F. Niedermayer, and P. Weisz, Nucl. Phys. **B367**, 123 (1991).
[24] A. Chodos and H. Minakata, Nucl. Phys. **B490**, 687 (1997).
[25] M. Mariño and T. Reis, J. High Energy Phys. 04 (2020) 160.
[26] L. Di Pietro, M. Mariño, G. Sberveglieri, and M. Serone, J. High Energy Phys. 10 (2021) 166.
[27] V. A. Fateev, V. A. Kazakov, and P. B. Wiegmann, Phys. Rev. Lett. **73**, 1750 (1994).
[28] V. Fateev, V. Kazakov, and P. Wiegmann, Nucl. Phys. **B424**, 505 (1994).
[29] V. Kazakov, E. Sobko, and K. Zarembo, Phys. Rev. Lett. **132**, 141602 (2024).
[30] M. Marino, R. Miravitllas, and T. Reis, arXiv:2302.08363.
[31] F. Gakhov, *Boundary Value Problems* (Dover Publications, New York, 1990).
[32] I. Gradshteyn and I. Ryzhik, *Table of Integrals, Series, and Products* (Elsevier Science, New York, 2014).